Polymer 50 (2009) 2572–2577

Contents lists available at ScienceDirect

Polymer

journal homepage: www.elsevier.com/locate/polymer

# Temperature-sensitive and highly water-soluble titanate nanotubes

Yuan Gao, Yongfeng Zhou*, Deyue Yan*

*School of Chemistry & Chemical Technology, Shanghai Jiao Tong University, 800 Dongchuan Road, Shanghai 200240, PR China*

ARTICLE INFO

*Article history:*
Received 3 September 2008
Received in revised form
6 April 2009
Accepted 10 April 2009
Available online 21 April 2009

*Keywords:*
Titanate nanotube
Temperature sensitive
ATRP

ABSTRACT

Water-soluble titanate nanotubes (TNTs) with temperature-responsive shells were synthesized by grafting poly(*N*-isopropylacrylamide) (PNIPAAm) from TNTs via surface atom transfer radical polymerization (ATRP) using ATRP agent functionalized TNTs as macroinitiator. Proton Nuclear magnetic resonance spectroscopy ($^1$H NMR), Fourier-transform infrared (FT-IR) and thermogravimetric analyses (TGA) results prove the successful graft of PNIPAAm chains from TNTs. TGA shows that the amount of PNIPAAm grown from the TNTs increased with the increase of monomer/initiator ratio. Transmission electron microscope (TEM) measurements displays the obtained TNTs-*g*-PNIPAAm nanohybrids have a core–shell structure of TNT cores and PNIPAAm shells. In addition, the functional nanotubes demonstrate a reversible low critical solution temperature (LCST) transition with the increase of solution temperature. The synthetic method presented here can also be extended to graft other stimuli responsive polymers from TNTs.



## 1. Introduction

In recent years, the researches about water-soluble nanohybrid materials based on nanoparticles [1], nanorods, nanotubes [2], etc. have attracted many attentions due to their extraordinary properties and widespread potential applications in biomaterials for tissue engineering, [3] biosensors, [4,5] bioelectronics [6] and dental/orthopedic implants [7]. An important issue in making these nano systems useful for specific applications is their capability to respond to external stimuli such as temperature and/or pH [8,9]. Thus, great efforts have been put into the preparation of intelligent water-soluble nanohybrids, which rapidly push the development of nanobioelectronics and nanobiotechnology [10–12]. For example, the integration of biomaterials (e.g., proteins/enzymes, antigens/antibodies, or DNA) with carbon nanotubes (CNTs) provide new hybrid systems that combine the conductive or semiconductive properties of nanomaterials with the recognition or catalytic properties of the biomaterials [13–16].

Compared with the CNTs, the titanate nanotubes (TNTs) [17–21] also possess high aspect ratio, uniform one-dimensional nano channel structure and larger surface area, but prevail due to their good properties including optical activity, ion-exchange property, lower toxicity and facile preparation in a large scale and cost-effective technology, especially their biocompatibility. However, the shortcomings of TNTs are also obvious including the high brittleness and bad solubility in water or organic matrix. Although, TNTs have hydrophilic surfaces, they tend to aggregate together in water within a short time and cannot be dispersed homogeneously into the biomaterials matrix, which greatly block their potential applications in biological systems. To break this limitation, organic functionalization of TNTs may be a good alternative. However, up to now, there are very few works concerning the organic functionalization of TNTs [22]. Very recently, our lab has reported the surface functionalization of TNTs with biodegradable poly(ε-caprolactone) (PCL) [23]. The obtained PCL-*g*-TNTs have demonstrated great improvements on the dispersibility and flexibility as well as a good biodegradable capacity.

Herein, we report a new way to prepare water-soluble and temperature-sensitive hybrid TNTs. Poly(*N*-isopropylacrylamide) (PNIPAAm) [24,25], one of the most often used thermoresponsive polymers in biotechnology and medicine, was successfully grafted to the surface of TNTs through an *in situ* ATPR technology. The obtained functional TNTs-*g*-PNIPAAm nanohybrids demonstrate excellent water solubility and reversible responsiveness to environmental temperature due to the thermo-sensitive phase transition of the coated PNIPAAm shells.

## 2. Experimental section

### 2.1. Materials

Titanate nanotubes were obtained from Institute of New Energy Material Chemistry Department of Material Chemistry, Nankai

* Corresponding authors. Tel.: +86 21 5474 2665; fax: +86 21 5474 1297.
*E-mail addresses:* yfzhou@sjtu.edu.cn (Y. Zhou), dyyan@sjtu.edu.cn (D. Yan).

0032-3861/$ – see front matter © 2009 Elsevier Ltd. All rights reserved.
doi:10.1016/j.polymer.2009.04.018

University, and the preparation is described in literature [26]. *N*-Isopropylacrylamide (NIPAAm), which was purchased from Aldrich, recrystallized from hexane at 60 °C. CuBr supplied by Shanghai Reagents Co. Ltd. was purified by stirring it overnight in absolute acetic acid. After filtration, it was washed with ethanol and diethyl ether and then dried. γ-aminopropyl triethoxysilane (γ-APS), 2-bromo-2-methyl-propionyl bromide (α-bromoisobutyryl bromide), *N*,*N*,*N*′,*N*″,*N*″-pentmethyldiethylenetriamine (PMDETA) were purchased from Acros and without purification. Acetone, methanol, ethanol, chloroform ($CHCl_3$) and other organic reagents or solvents were obtained from domestic market; they were previously distilled and kept in the presence of 4 Å molecular sieve to eliminate any traces of water before use.

### 2.2. Instrumentation

FT-IR is conducted on a Perkin–Elmer Paragon 1000 instrument. All samples are prepared as pellets using spectroscopic grade KBr. Ultraviolet–Visible (UV–Vis) spectra were measured on a GBC Cintra 10e UV visible spectrophotometer equipped with a thermal cell. $^1$H NMR measurements are performed on a Varian Mercury plus-400 spectrometer; TMS is used as the internal reference. TGA is carried out on a Perkin–Elmer TGA-7 instrument with a heating rate of 20 °C/min in a nitrogen flow (20 mL/min). DSC studies were performed from 10 to 60 °C (heating rate 5 °C/min) on a Q1000 modulated DSC (TA Instruments) under a nitrogen atmosphere. TEM studies are performed on a JEOL JEM-2100F instrument operating at a voltage of 200 kV. Samples are prepared by dropping the sample solutions onto carbon-coated copper grids and air-dried before measurement. SEM images were recorded using an FEI SIRION200 field emission scanning electron microscope, and the samples were loaded on the silicon surface, previously sputter-coated with a homogeneous gold layer for charge dissipation during the SEM imaging. AFM studies (tapping mode) were performed using a Multimode Nanoscope IIIa scanning probe microscope with a standard silicon nitride cantilever. X-ray photoelectron spectroscopy (XPS) spectra were recorded with a PerkinElmer PHI 5000C system equipped with a hemispherical electron energy analyzer. The Mg Kα ($h\upsilon = 1253.6$ eV) was operated at 15 kV and 20 mA. The Binding energy (BE) was calibrated by using the containment carbon (C 1s = 284.6 eV).

### 2.3. Synthesis of brominated TNTs

5.0 g TNTs were added to 100 mL of anhydrous toluene under $N_2$ atmosphere in a 250 mL flask with a reflux condenser. γ-APS was injected into the reaction system and refluxed at 80 °C for 24 h. The resultant was ultrasonically washed with toluene and acetone to remove any unreacted silane coupling agents. The APS modified TNTs (TNTs–$NH_2$) were obtained and dried under vacuum. Then TNTs–$NH_2$, anhydrous $CH_2Cl_2$ and triethylamine were added into a 150 mL flask. Then $CH_2Cl_2$ solution of 2-bromo-2-methyl-propionyl bromide was added dropwise at 0 °C within 1 h. The mixture was stirred for 3 h at 0 °C, followed by stirring at room temperature for 48 h. The resultant brominated TNTs (TNTs–Br) were obtained and washed with $CH_2Cl_2$ and dried under vacuum. The FT-IR and X-ray photoelectron spectroscopy (XPS) spectra were used to characterize the organically modified TNT. Bromine content of TNTs–Br was determined by element analysis, TGA, and Energy-dispersion X-ray (EDX) spectroscopy to be 0.281 mmol/g.

### 2.4. Grafting PNIPAAm from the surface of TNTs

Typically, 25.2 mg of brominated TNTs, 7.2 mg (0.050 mmol) of CuBr, 8.7 mg (0.050 mmol) of PMDETA and 0.5 mL of pure water were placed into a 10 mL dried flask and sealed with a rubber plug. The flask was evacuated and back-filled with Ar-gas three times to remove any trace of oxygen. After this procedure, a certain amount of NIPAAm dissolved in 0.5 mL of degassed water was injected into the flask using a syringe. The flask was kept at room temperature and stirred for 48 h. The final products were purified by ultrasonic dispersion and centrifugation for five times in water to ensure the removing of resultant homopolymers completely, and drying overnight under vacuum to obtain the white powder. Evidence for the successful graft was provided by FT-IR, $^1$H NMR, TEM images, and TGA measurement.

## 3. Results and discussion

There is a large amount of Ti–OH groups existing on the surface of TNTs and they provide the potentiality to modify the TNTs with organosilanes. Thus, the inorganic hydroxyl groups with low reactivity on surface of TNTs are transformed into the more reactive organic functional groups for further functionalization. Our strategy to modify TNTs is described in Scheme 1. Firstly, organic amino groups were introduced onto the surface of TNTs by the reaction of organosilane (APS) with hydroxyl-contained titanate nanotubes [27,28]. Secondly, initiating sites (TNTs–Br) for ATRP were formed by reacting amine-modified TNTs with 2-bromo-2-methylpropionyl bromide. Thirdly, grafting polymerization of NIPAAm from TNTs–Br was carried our by means of *in situ* ATRP, resulting in TNTs-*g*-PNIPAAm. Representative reaction conditions of ATRP are provided in Table 1. Three hybrid TNT samples, denoted as TP1 to TP3, were prepared and carefully characterized.

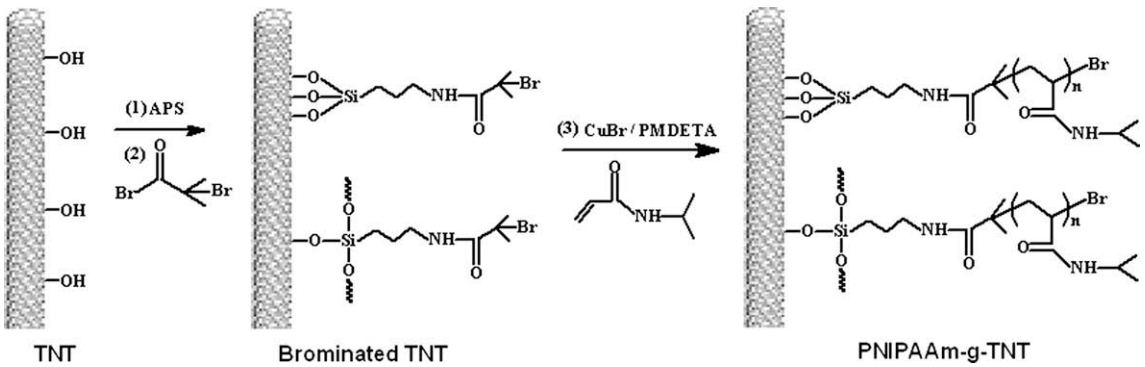


**Scheme 1.** Schematic illustration of the synthesis of PNIPAAm-*g*-TNT. Only two representative coupling reactions between APS and Ti–OH groups or those between APS were illustrated for simplicity.

**Table 1**
The reaction conditions and some results.

| Sample | R[a] | $f$[b] (wt/%) | $d$[c] (nm) |
|---|---|---|---|
| TP1 | 13:1 | 30 | $3.3 \pm 0.02$ |
| TP2 | 65:1 | 45 | $6.04 \pm 0.04$ |
| TP3 | 130:1 | 60 | $10.25 \pm 0.25$ |

[a] R = monomer:brominated TNTs (wt:wt).
[b] $f_{wt}$ = the weight content of grafted PNIPAAm in the nanohybrids calculated from TGA data.
[c] $d = \bar{d} \pm \sigma\bar{d}$, is the average thickness of grafted polymer layers calculated through a statistic analysis of ten nanotubes measured from TEM images, and $\sigma$ is the standard deviation of thickness.

FT-IR (Fig. 1) and XPS (Fig. 2) spectra were used to characterize the organically modified TNTs. In the FT-IR spectrum of TNTs–$NH_2$ (Fig. 1b), 2900 $cm^{-1}$ (the stretching vibration of C–H groups), 1442 $cm^{-1}$ (the bending vibration of C–H groups), 1095 $cm^{-1}$ (the Si–O groups), 3380 and 3301 $cm^{-1}$ (the $NH_2$ groups) could be clearly detected. It indicates the successful anchoring of APS groups onto the surface of TNTs.

Compared with TNTs–$NH_2$, the FT-IR spectrum (Fig. 1c) of TNTs–Br demonstrates the characteristic absorption bands occurred at 1680 $cm^{-1}$ and 1100–1200 $cm^{-1}$ (the amide groups), and 690 $cm^{-1}$ (the C–Br groups) [29]. XPS (Fig. 2) spectra provide more detailed evidences to prove that bromide groups have been grafted onto the surface of TNTs successfully. In the XPS spectra of TNTs–Br, the characteristic peaks of Br 3d were found around 104.3 eV. In addition, the binding energy of Ti 2p3/2 shifts from 458.24 to 457.9 eV (Fig. 2, inset), which is ascribed to a decrease in the positive charge on Ti atoms because of the formation of Ti–O–Si bonds at the TNTs surface. Thus, it can be concluded that by modifying pristine TNTs with APS and 2-bromo-2-methylpropionyl bromide, the inert inorganic TNTs have been changed into functional hybrid nanotubes with many ATRP initiators.

The TNTs-*g*-PNIPAAm were prepared via *in situ* ATRP of NIPAAm monomers from the surface of TNTs–Br. The FT-IR spectrum (Fig. 1d) of the TNTs-*g*-PNIPAAm shows characteristic peaks for grafted PNIPAAm (C–H groups at 2970, 1450, and 1366 $cm^{-1}$, C=O groups at 1650 $cm^{-1}$, N–H at 3300 and 1550 $cm^{-1}$). In addition, $^1$H NMR spectrum of TNTs-*g*-PNIPAAm provides more detailed evidences (Fig. 6, 20 °C). The characteristic peaks of PNIPAAm, such as the peak at $\delta = 3.9$ ppm (peak c) ascribed to CONH–*CH* ($CH_3$)–$CH_3$, and the peak at $\delta = 1.1$ ppm (peak d) ascribed to CONH–CH ($CH_3$)–$CH_3$, and $\delta = 3.9$ ppm (peaks a and b) ascribed to –$CH_2$–*CH* (CONH)–, were clearly found. All these results strongly support that PNIPAAm have been successfully grafted from brominated TNTs by ATRP.

The merit of the ATRP approach is the possibility to introduce uniform coatings on TNTs. Here we have succeeded in evenly wrapping PNIPAAm on the TNTs surface, and this has been confirmed by TEM observations. Fig. 3a displays a typical TEM image of pristine TNTs obtained by a hydrothermal reaction. The tubes possess uniform inner and outer diameters of about 6–7 and 10–12 nm in average along their length, respectively, and the average length is about several hundreds of nanometers. They are multilayered and open-ended, and have a smooth surface. The PNIPAAm-coated TNTs can be easily distinguished from pristine TNTs as both the polymer shell and the TNTs crystal sheet structures are clearly discerned as shown in Fig. 3b–d. We have measured the polymer shell thickness from the TEM images, and the thickness in average for each PNIPAAm-*g*-TNT sample was obtained through a statistical analysis of ten nanotubes. With the increase of monomer feed ratio, the thickness of the grafted polymer shell varies from $3.30 \pm 0.02$, $6.04 \pm 0.04$ to $10.25 \pm 0.25$ nm (Table 1). The shell thickness is very uniform when the TNTs were grafted with a lower PNIPAAm content (Fig. 3b and c), indicating a well controllability of the ATRP reaction. However, when the PNIPAAm content is much higher, there is a bigger derivation in the shell thickness. Both the uneven (Fig. 3d) and uniform (Fig. 3d, inset) TNTs-*g*-PNIPAAm were obtained.

Furthermore, the result of TEM measurements is well consistent with that obtained from TGA analyses (Fig. 4). The TGA curves show a major decomposition in the temperature range at 225–450 °C, which should be attributed to the thermal degradation of PNIPAAm polymers coated on the TNTs when compared to the TGA curve of PNIPAAm polymers (Fig. 4e). Thus, the PNIPAAm content in TNTs-*g*-PNIPAAm can be calculated (Table 1), and it is 30% for TP1, 45% for TP2, and 60% for TP3, respectively. These results further indicate that the content of the grated polymer in the functionalized TNTs can be adjusted by monomer/initiator ratio.

The possibility of temperature switching behavior of the as-prepared TNTs-*g*-PNIPAAm in aqueous solution was also evaluated. The sample was fully dispersed in water, forming a stable milky solution at room temperature for more than one week. However,

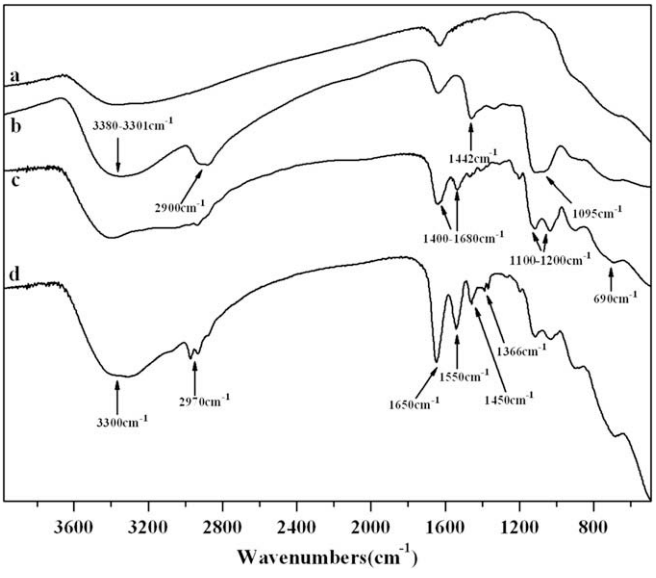


**Fig. 1.** The FT-IR spectra of pristine TNTs (a); TNTs–$NH_2$ (b); TNTs–Br (c); TNTs-*g*-PNIPAAm (d).

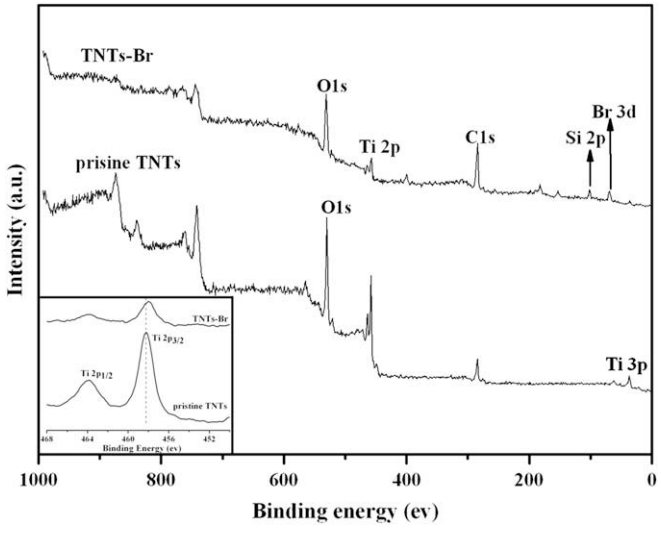


**Fig. 2.** Wide scan XPS spectra of the pristine TNTs and TNTs–Br (inset, high-resolution XPS spectra of Ti 2p spectra).

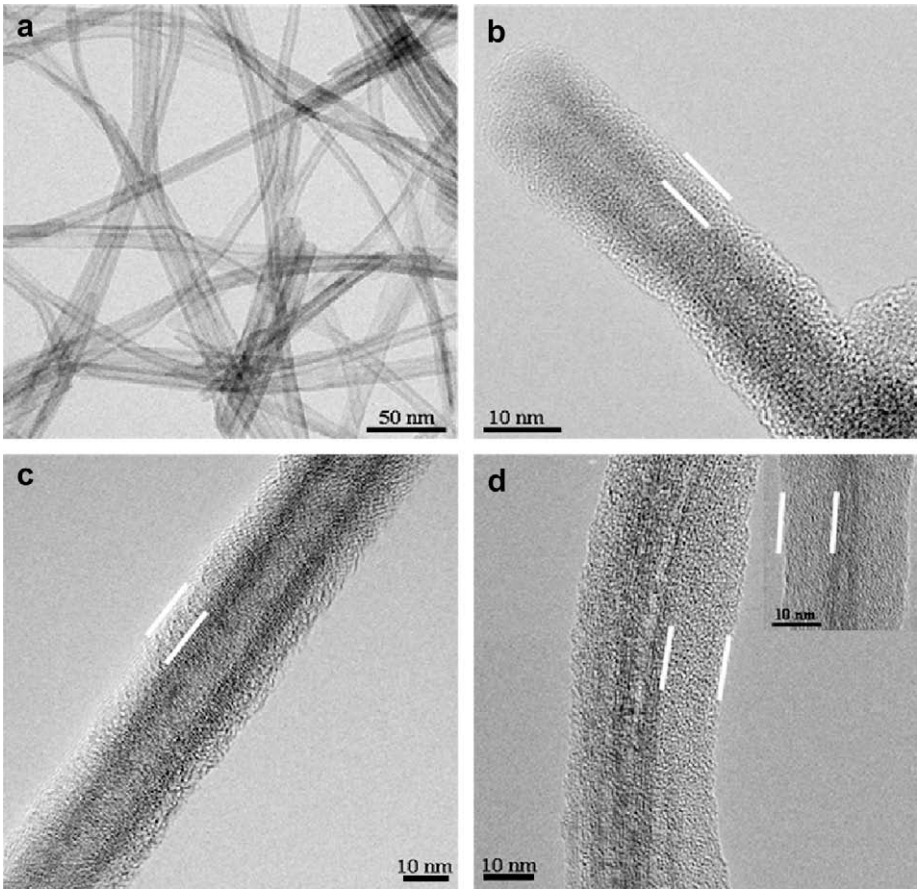


**Fig. 3.** TEM images of pristine TNTs (a), TP1 (b), TP2 (c), and TP3 (d).

with the temperature increasing to 35 °C, the hybrids gradually precipitated from aqueous solution. Such a temperature-responsive solubility of the nanohybrids is reversible. When the temperature was lowered, the precipitation dispersed again to form a homogeneous solution. This tests preliminary proved that TNTs-*g*-PNIPAAm have the thermally responsive property.

Furthermore, such temperature sensitive behavior of PNIPAAms' solubility in water was determined by temperature-controlled UV–Vis spectroscopy. Fig. 5 displays the absorbance of TNTs-*g*-PNIPAAm (TP2) at 250 nm as a function of temperature in aqueous solution. The absorbance of TNTs-*g*-PNIPAAm almost remains a constant below 30 °C, but it gradually decreases until 45 °C, and then remains invariable again with increasing temperature. It was found that the transition temperature midpoint is 34 °C, which is

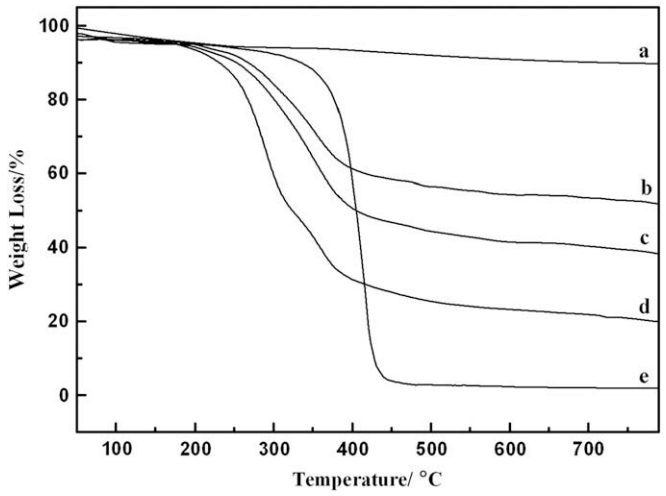


**Fig. 4.** The TGA curves of pristine TNTs (a), TNTs-*g*-PNIPAAm with different NIPAAm feed ratio (TP1–TP3) (b–d) and pure PNIPAAm (e).

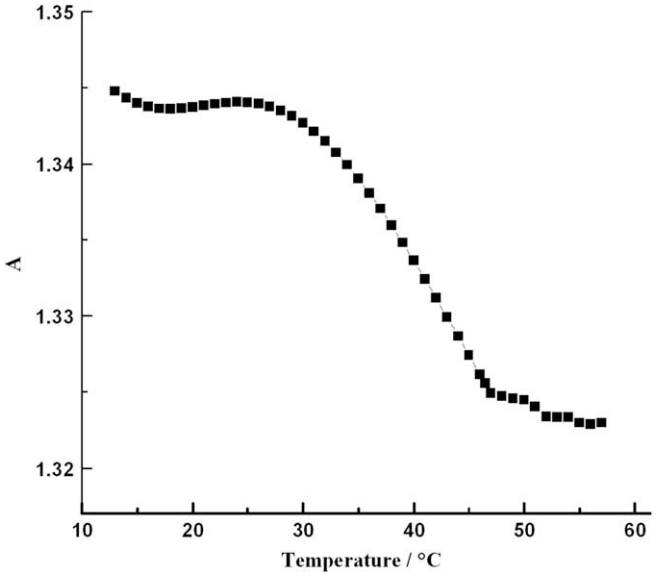


**Fig. 5.** The absorbance of TNTs-*g*-PNIPAAm in water as a function of temperature.

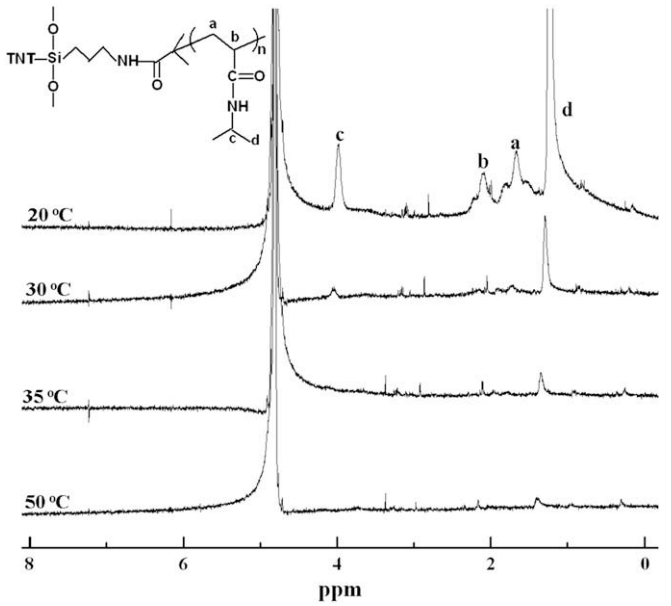


**Fig. 6.** $^1$H NMR spectra of NIPAAm-*g*-TNTs in $D_2O$ at different temperature.

higher than the low critical solution temperature (LCST) of pure PNIPAAm (~32 °C) [21]. Meanwhile, we can also observe in Fig. 5 that the phase transition range, from 30 °C to 45 °C, is wider than that of pure PNIPAAm as well as the PNIPAAm-*g*-CNTs [30]. Generally, the LCST phase transition is due to the coil-to-globe conformation transition of the grafted PNIPAAm brushes in water with increasing temperature [31]. TNTs are more rigid than CNTs, and will strongly prohibit the conformation tumbling of the coated polymers, which induces a slow LCST transition.

We also use temperature-variable $^1$H NMR to detect the temperature sensitive property of the TNTs-*g*-PNIPAAm. Fig. 6 shows the $^1$H NMR spectra of TNTs-*g*-PNIPAAm in $D_2O$ at 20, 30, 35, and 50 °C respectively. The corresponding proton signals of PNIPAAm chains (peaks a–d) can easily be observed at 20 °C. With the increasing of temperature to 30 °C, the signals become weaker but could still be detected clearly. When the temperature was increased to at 50 °C, all the signals of PNIPAAm chains can hardly be detected. The results further support the conformation transformations of TNTs-*g*-PNIPAAm from a hydrophilic state into a hydrophobic one. At temperature above 30 °C, intramolecular hydrogen bondings are formed between C=O and amine groups in the PNIPAAm chains, while the intermolecular hydrogen bondings between PNIPAAm and water are partly broken, thus the PNIPAAm chains at the surface change from a coil conformation into a densely aggregated structure, which makes the polymer hybrids insoluble in water. At an even higher temperature, the polymer coated TNTs precipitate from water almost completely, so the PNIPAAm units cannot be clearly detected in NMR spectrum.

The hydrophilic/hydrophobic phase transition of TNTs-*g*-PNIPAAm can induce endo- or exo-thermal effects, which can be detected by DSC. Fig. 7 shows a clear endo peak around 34 °C for aqueous sample of TP2, indicating that the switching of aggregate and disaggregate of TNTs-*g*-PNIPAAm in water can be controlled through the temperature variation. Compared to the UV measurement, the thermosensitive phase transition detected by DSC is sharper and was completed in a temperature range from 32 to 37 °C. The reasons for the difference between DSC and UV measurements lie in the higher sensitivity of modulated DSC used in this experiment and a higher temperature-heating rate. These results further demonstrate that the PNIPAAm chains coated on TNTs still preserve the temperature-responsive ability.

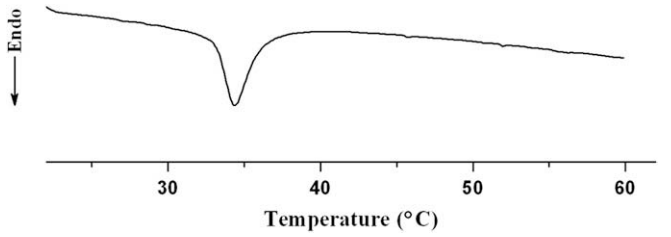


**Fig. 7.** DSC thermogram of NIPAAm-*g*-TNTs (TP2) in water at heating rate of 5 °C/min.

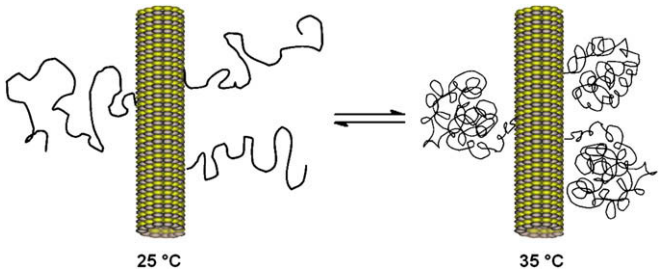


**Scheme 2.** Schematic illustration for conformation change of PNIPAAm chains on TNT.

Based on the results of above measurements, a mechanism for the thermally responsive behavior of TNTs-*g*-PNIPAAm nanocomposites is presented in Scheme 2. At temperatures below the LCST, the intermolecular hydrogen bonding between the PNIPAAm chains and water molecules plays a dominant role, and the PNIPAAm chains are in a loosely coil structure and soluble in water. At temperature above LCST, the graft PNIPAAm chains dehydrate to form a compact globe structure, which makes the PNIPAAm chains insoluble in water and precipitate from the solution.

## 4. Conclusions

In conclusion, PNIPAAm was covalently grafted onto the TNTs convex surfaces by an *in situ* ATRP technology, resulting in core–shell nanocomposites with various contents of uniform polymer layers. The thickness of the grafted polymer shell is adjustable by the control of the monomer/initiator ratio. The larger is the monomer/initiator ratio, the thicker is the polymer shell. The TNTs-*g*-PNIPAAm showed temperature-switching assembly and disassembly behaviors in water, because of the hydrophilic and hydrophobic transformation of the grafted PNIPAAm chains. It is anticipated that such nanocomposites, with good mechanical properties and good thermo-sensitivity, are potential to be used in shape memory materials, artificial muscles, and controllable drug-delivery. In addition, this surface ATRP method presented here can be extended to graft other stimuli responsive polymers from TNTs.

## Acknowledgments

This work was supported by the Special Funds for Major State Basic Research Projects (2005CB623803), the National Natural Science Foundation of China (No. 2009CB930400, 2007CB808000), the National Natural Science Foundation of China (No. 50633010, 20774057, 20874060 and 50873058), the Program for New Century Excellent Talents in University (NCET-07-0558), the Foundation for the Author of National Excellent Doctoral Dissertation of China, the Fok Ying Tung Education Foundation (No. 114029), the Basic Research Foundation (07DJ14004) of Shanghai Science and Technique Committee, and the Shanghai Leading Academic Discipline Project (B202). We also thank the Instrument Analysis Center of SJTU for providing the measurement.

## References


[1] Tang ZY, Zhang ZL, Wang Y, Glotzer SC, Kotov NA. Science 2006;314:274–8.
[2] Feng L, Li SH, Li YS, Li HJ, Zhang LJ, Zhai J, et al. Adv Mater 2002;14:1857–60.
[3] Shi X, Hudson JL, Spicer PP, Tour JM, Krishnamoorti R, Mikos AG. Biomacromolecules 2006;7:2237–42.
[4] Willner I. Science 2002;298:2407–8.
[5] Xiao Y, Patolsky F, Katz E, Hainfeld JF, Willner I. Science 2003;299:1877–81.
[6] Baughman RH, Zakhidov AA, de Heer WA. Science 2002;297:787–92.
[7] Li H, Chen Y, Xie Y. Mater Lett 2003;57:2848–54.
[8] Barone PW, Strano MS. Angew Chem Int Ed 2006;45:8138–41.
[9] Xu YY, Bolisetty S, Drechsler M, Fang B, Yuan JY, Ballauff M, et al. Polymer 2008;49:3957–64.
[10] Niemeyer CM. Angew Chem Int Ed 2001;40:4128–58.
[11] Niemeyer CM. Angew Chem Int Ed 2003;42:5796–800.
[12] Parak WJ, Gerion D, Pellegrino T, Zanchet D, Micheel C, Williams SC, et al. Nanotechnology 2003;14:R15–27.
[13] Dai L, He P, Li S. Nanotechnology 2003;14:1081–97.
[14] Pantarotto D, Briand JP, Prato M, Bianco A. Chem Commun 2004;10:16–7.
[15] Wong SS, Joselevich E, Woolley AT, Cheung CL, Lieber CM. Nature 1998;394:52–5.
[16] Hafner JH, Cheung CL, Woolley AT, Lieber CM. Prog Biophys Mol Biol 2001;77:73–110.
[17] Kasuga T, Hiramatsu M, Hoson A, Sekino T, Niihara K. Adv Mater 1999;11:1307–11.
[18] Seo DS, Lee JK, Kim H. J Cryst Growth 2001;229:428–32.
[19] Chen Q, Zhou WZ, Du GH, Peng LM. Adv Mater 2002;14:1208–11.
[20] Zhang S, Peng LM, Chen Q, Du GH, Dawson G, Zhou WZ. Phys Rev Lett 2003;91:2561031–4.
[21] Zhang QH, Gao L, Zheng S, Sun J. Chem Lett 2002;2:226–7.
[22] Byrne MT, McCarthy JE, Bent M, Blake R, Gun'ko YK, Horvath E, et al. J Mater Chem 2007;17:2351–8.
[23] Shi ZQ, Gao XP, Song DY, Zhou YF, Yan DY. Polymer 2007;48:7516–22.
[24] Schild HG. Prog Polym Sci 1992;17:163–249.
[25] Sun TL, Wang FJ, Feng L, Liu BQ, Ma YM, Jiang L, et al. Angew Chem Int Ed 2004;43:357–60.
[26] Gao XP, Lan Y, Zhu HY, Liu JW, Ge YP, Wu F, et al. Electrochem Solid-State Lett 2005;8:A26–9.
[27] Brunel D, Bellocq N, Sutra P, Cauvel A, Laspéras M, Moreau P, et al. Coord Chem Rev 1998;178–180:1085–103.
[28] Fadeev AY, McCarthy TJ. Langmuir 2000;16:7268–74.
[29] Moc J. Chem Phys 1999;247:365–73.
[30] Kong H, Li W, Gao C, Yan D, Jin Y, Walton DRM, et al. Macromolecules 2004;37:6683–6.
[31] Gil ES, Hudson SM. Prog Polym Sci 2004;29:1173–222.